cluster. On the basis of the homology between the mammalian and crustacean proteins,[20,22] given in Figure 1, and the presence of two independent three-metal clusters,[21] we expect that each cluster in crab and lobster (l) MTs will also be located in a distinct domain (hereafter designated β_c or β_n, referring to the ends of the protein sequence). We are able to predict the structure (Cd–S connections) of l-MT (Figure 6), on the basis of these homologies and the structural patterns found for the m-MTs.[11-13] Eight of the nine cysteines in the N-terminal region of l-MT correspond to cysteines of the mammalian β-cluster. One is missing and is replaced by a new cysteine later in the sequence. Eight of the eleven cysteines of the m-α-domain are present in the C-terminal sequence of l-MT; three are absent, and one new one appears. For each lobster MT domain, the "conserved" residues easily bind to a three-metal cluster, conserving the protein loop sizes ($\Delta n \pm 0$, 1, or 2, where Δn is the number of intervening peptide bonds).

In the l-β_n-domain, there is no residue corresponding to m-CYS-19, but a new residue, l-CYS-27 appears.[20,22] m-CYS-19 is bound to Cd-2 (Figure 6, Cds numbered according to the ^{113}Cd NMR spectra for m-MTs).[11-13] The new residue l-CYS-27 is one residue removed from l-CYS-25, which is homologous to m-CYS-29 that also binds to Cd-2. Binding to the same cadmium by cysteines that are adjacent ($\Delta n = 1$) or one residue removed ($\Delta n = 2$) from one another is a common motif. Thus we propose that l-CYS-27 "replaces" m-CYS-19 as ligand to Cd-2 and that all other cysteines follow the pattern of m-MT. As shown on the left side of Figure 6, the protein loops (Δn) between metal–thiolate connections remain relatively unchanged between the mammalian and lobster clusters.

The mammalian α-domain has two types of Cd(II) ions, those with two terminal cysteines (Cd-1 and Cd-5) and those with only one (Cd-6 and Cd-7).[9,11-13] This structure can be "generated" by adding a fourth cadmium with two terminal ligands and converting two previously-terminal ligands of the three-metal cluster into bridging ligands. Thus, removing either Cd-5 or Cd-1 and their terminal thiols leaves three Cds and nine thiolate ligands arranged as three-metal clusters. Interestingly, two (of the three) cysteines omitted in the l-β_c-domain,[20,22] m-CYS-33 and -48, are ligands to Cd-5.[11-13] Thus, we propose that the l-β_c-domain is constructed with the homologous cysteines connected to Cd-1, -6, and -7, with the new l-CYS-49 replacing the missing m-CYS-36 as a ligand to Cd-7. Stout et al.[11] have also predicted that Cd-5 is likely to be omitted in crab MT.

At present, there is no evidence that the domains function in concert with one another. In the reactions of either the mammalian[17] or lobster proteins (this work) with DTNB, the domains react independently. Yet the hinge regions that connect the domains are precisely conserved in length and nature of the residues among the mammalian MTs (–K–K–S–, residues 30–32) and among the crustacean MTs (–A/S/P–P–, residues 28–29), although not between the two types. Thus, it is not clear whether there is a requirement for precise positioning of the metal clusters relative to one another. If the l-CYS-25 and -27 residues are positioned as shown in Figure 6, the hinge region begins in a stereochemical configuration that is different for lobster and mammalian MTs. If residues 25 and 27 are switched in position, then l-CYS-27 occupies the coordination site corresponding to m-CYS-29, each being the last cysteine of the corresponding domains. CYS-33, the first in the m-α-domain is not present in the lobster β_c-domain since Cd-5 is missing, and this difference may dictate that, in any event, the domains are oriented differently in mammalian and crustacean MTs.

Registry No. DTNB, 69-78-3.

Contribution from the Departamento de Quimica Inorgânica, Facultad de Quimica, Universidad de Valencia, 46100 Burjasot, Spain

Magnetic Characterization of Tetranuclear Copper(II) and Cobalt(II) Exchange-Coupled Clusters Encapsulated in Heteropolyoxotungstate Complexes. Study of the Nature of the Ground States

Carlos J. Gômez-Garcia, Eugenio Coronado,* and Juan J. Borrâs-Almenar

Received July 26, 1991

This paper presents a magnetic characterization of the heteropolyanions $[M_4(H_2O)_2(PW_9O_{34})_2]^{10-}$ and $[M_4(H_2O)_2(P_2W_{15}O_{56})_2]^{16-}$ (M = Cu(II), Co(II)), with emphasis on the exchange interactions. Their individual heteropolyoxometalate molecules encapsulate a rhomblike arrangement formed by four coplanar MO_6 octahedra sharing edges. The magnetic susceptibility data show that the four copper ions are antiferromagnetically coupled, while in the cobalt(II) complexes the intramolecular exchange is ferromagnetic. In all cases the ground state of the M_4O_{16} molecules has been found to be magnetic. These behaviors are discussed from isotropic (Cu_4 clusters) or anisotropic (Co_4 clusters) exchange models. In case of copper compounds, the presence of a triplet ground state is in agreement with the order of energy levels deduced from the analysis of the magnetic data and is confirmed from EPR and magnetization measurements. This intermediate-spin ground state is discussed in relation with spin frustration resulting from the presence of two competing copper–copper interactions in the rhomb. Finally, the nature of the ground state as well as the presence of intercluster interactions in the cobalt clusters are examined from low-temperature susceptibility and magnetization measurements and compared with the results obtained in the copper clusters.

Introduction

Polyoxometalate complexes resemble discrete fragments of metal oxide structures of definite sizes and shapes, which maintain their identities in solution as well as in the solid state.[1-3] In view of their topological and electronic structural versatility this class of inorganic compounds attracts current attention in analytical chemistry, catalysis, biology, medicine, geochemistry, topology and materials science.

These kinds of compounds have attracted our attention as model systems for the study of magnetic exchange interactions in clusters but also for use as components of new magnetic molecular materials. With respect to the former aspect, the magnetic properties of these compounds have been little studied up to now, due probably to the weak magnetism of the samples (the magnetic sites are encapsulated in a diamagnetic molecular metal oxide cluster). Nevertheless, they can be especially valuable in this area

(1) Pope, M. T. *Heteropoly and Isopoly Oxometalates*; Springer-Verlag: Berlin, 1983.
(2) Pope, M. T.; Muller, A. *Angew. Chem., Int. Ed. Engl.* **1991**, *30*, 34.
(3) Baker, L. C. W. *Advances in the Chemistry of the Coordination Compounds*; Kirschner, S., Ed.; MacMillan: New York, 1961; p 608.

0020-1669/92/1331-1667$03.00/0

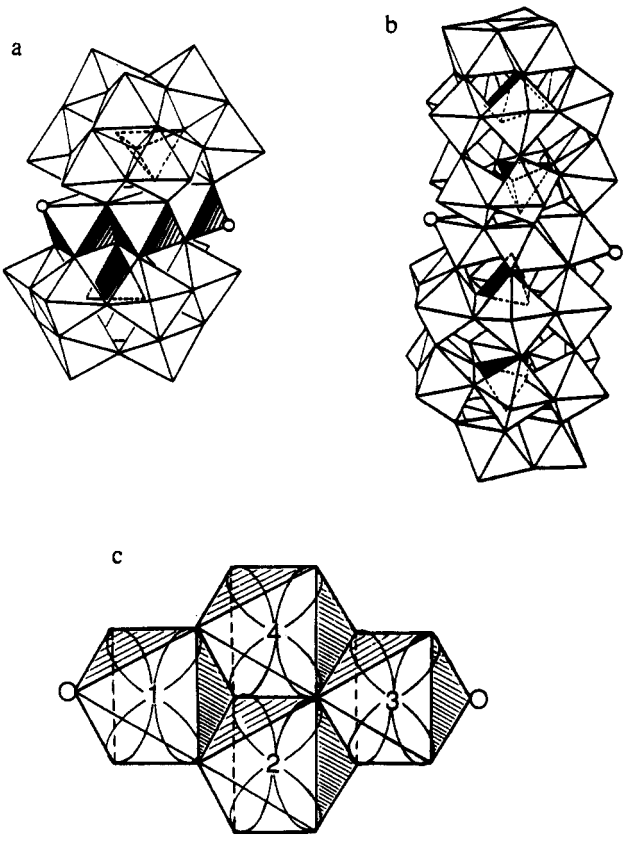

Figure 1. Structures of the $[M_4(H_2O)_2(PW_9O_{34})_2]^{10-}$ (Keggin derivative) (a) and $[M_4(H_2O)_2(P_2W_{15}O_{56})_2]^{16-}$ (Dawson–Wells derivative) (b) complexes. Each vertex of a polyhedron locates the center of an O atom. Each white octahedron contains a W atom. Each tetrahedron contains a P atom. Each shaded octahedron contains a M atom. (c) Geometry of the magnetic moiety M_4O_{16}, showing the orientation of the $d_{x^2-y^2}$ metal orbitals in the copper clusters. The circles locate the O atoms of the H_2O molecules coordinated to two of the M's.

since they offer ideal structural supports for the study of the interactions between paramagnetic metal atoms[4,5] as well as between delocalized electrons and paramagnetic metal atoms.[6] With respect to the applications in materials science, diamagnetic polyoxoanions have been used very recently as inorganic electron-acceptor components in charge-transfer salts, using π-donor organic radicals as cations.[7,8] To our knowledge no studies have been reported in this context using magnetic polyoxoanions.

In previous studies[9,10] we have reported the magnetic behaviors of cobalt(II) and copper(II) tetrameric clusters of the series $[M_4(H_2O)_2(PW_9O_{34})_2]^{10-}$ in the temperature range 5–100 K. An analysis of the cobalt data on the basis of an anisotropic exchange model developed in ref 9 allowed us to calculate a ferromagnetic in-cluster cobalt-cobalt interaction $2J_{\parallel} = 19$ cm^{-1} with an amount of exchange anisotropy in the range 0.1–0.5. On the other hand, the magnetic behavior of the copper complex was modeled on the basis of a Heisenberg exchange model.[10] No evidence of intercluster exchange interactions was found in these two compounds from these data.

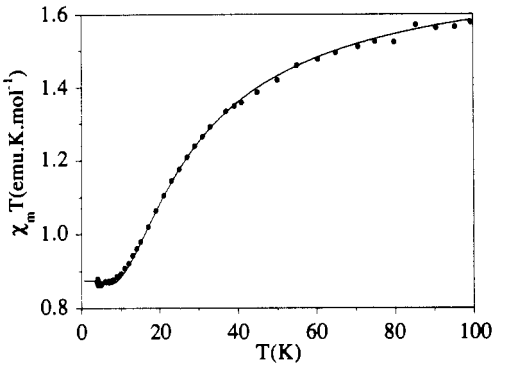

Figure 2. Plot of $\chi_m T$ versus T for the Keggin derivative copper compound I. The solid line represents the best fit from the Heisenberg exchange model.

To complete the magnetic characterization of these clusters, we report in this paper the magnetic properties down to 2 K, together with low-temperature magnetization and EPR results. These measurements have shown to provide useful information on intercluster exchange interactions and on the nature of the magnetic ground state of the clusters. On the other hand, we also report the magnetic characterization of the related polyoxoanions $[M_4(H_2O)_2(P_2W_{15}O_{56})_2]^{16-}$ (M = Cu(II), Co(II)).

All these anions contain isolated polymetallic clusters M_4O_{16} between two diamagnetic anions $(PW_9O_{34})^{9-}$ (Figure 1a) or $(P_2W_{15}O_{56})^{12-}$ Figure 1b), derived from Keggin[11] and Dawson–Wells[12] structures, respectively. The high symmetry of the tetrameric cluster M_4O_{16} is determined by the rigidity of the tungstophosphate ligands, $(PW_9O_{34})^{9-}$ or $(P_2W_{15}O_{56})^{12-}$, which imposes a rhomblike centrosymmetric arrangement with C_{2h} symmetry formed by four coplanar MO_6 octahedra sharing edges (see Figure 1c). This magnetic cluster shares seven oxygen atoms with each tungstophosphate ligand. The two unshared MO_6 vertices are coordinated to water ligands. When comparing the exact geometries of these clusters, we notice that the only significant difference is the marked Jahn–Teller axial distortion of the CuO_6 octahedra[13] in contrast with the smaller distortions in the CoO_6 octahedra.[14] Thus, in copper compounds the long axes within each anion are parallel. This fact will be important when the magnetic interactions between the copper atoms are discussed.

Experimental Section

The compounds $K_8Na_2[Cu_4(H_2O)_2(PW_9O_{34})_2]\cdot 16H_2O$ (I), $Na_{16}[Cu_4(H_2O)_2(P_2W_{15}O_{56})_2]\cdot 44H_2O$ (II), $K_{10}[Co_4(H_2O)_2(PW_9O_{34})_2]\cdot 23H_2O$ (III), and $Na_{16}[Co_4(H_2O)_2(P_2W_{15}O_{56})_2]\cdot 51H_2O$ (IV), prepared and recrystallized as previously described,[15] were characterized by IR spectroscopy and X-ray powder diffraction. The analysis of the magnetic ions are in agreement with the presence of four metallic atoms per formula. (Calc for I: Cu, 4.71. Found: Cu, 4.70. Calc for II: Cu, 2.80. Found: Cu, 2.80. Calc for III: Co, 4.26. Found: Co, 4.40. Calc for IV: Co, 2.65. Found: Co, 2.70.) The degree of hydration (%) for these compounds was determined by TGA measurements and is in good agreement with previous reports.[15] (Calc for I: H_2O, 6.18. Found: 6.07. Calc for II: H_2O, 10.93. Found: 10.98. Calc for III: H_2O, 8.13. Found: 8.30. Calc for IV: H_2O, 9.30. Found: 9.26.)

(4) Kokoszka, G. F.; Padula, F.; Goldstein, A. S.; Venturini, E. L.; Azevedo, L.; Siedle, A. R. *Inorg. Chem.* **1988**, *27*, 59.
(5) (a) Simmons, V. E. Doctoral Dissertation, Boston University, 1963; *Diss. Abstr.* **1963**, *24*, 1391. (b) Baker, L. C. W.; Baker, V. E. S.; Wasfi, S. H.; Candela, G. A.; Kahn, A. H. *J. Am. Chem. Soc.* **1972**, *94*, 5499. (c) Baker, L. C. W.; Baker, V. E. S.; Wasfi, S. H.; Candela, G. A.; Kahn, A. H. *J. Chem. Phys.* **1972**, *56*, 4917.
(6) Casañ-Pastor, N. Doctoral Dissertation, Georgetown University, 1988.
(7) (a) Ouahab, L.; Bencharif, M.; Grandjean, D. *C. R. Acad. Sci. Paris, Ser. 2* **1988**, *307*, 749. (b) Mhanni, A.; Ouahab, L.; Pena, O.; Grandjean, D.; Garrigou-Lagrange, C.; Delhaes, P. *Synth. Met.* **1991**, *41–43*, 1703. (c) Triki, S.; Ouahab, L.; Grandjean, D.; Fabre, J. M. *Acta Crystallogr.* **1991**, *C47*, 645. (d) Triki, S.; Ouahab, L.; Pandiou, J.; Grandjean, D. *J. Chem. Soc., Chem. Commun.* **1989**, 1068.
(8) Bellitto, C.; Attanasio, D.; Bonamico, M.; Fares, V.; Imperatori, P.; Patrizio, S. *Mat. Res. Soc. Proc.* **1990**, *173*, 143. (b) Davidson, A.; Boubekeur, K.; Pénicaud, A.; Auban, P.; Lenoir, C.; Batail, P.; Hervé, G. *J. Chem. Soc., Chem. Commun.* **1989**, 1373.
(9) Casañ-Pastor, N.; Bas-Serra, J.; Coronado, E.; Pourroy, G.; Baker, L. C. W. *J. Am. Chem. Soc.*, in press.
(10) Gómez-Garcia, C. J.; Casañ-Pastor, N.; Coronado, E.; Baker, L. C. W.; Pourroy, G. *J. Appl. Phys.* **1990**, *67*, 5995.
(11) (a) Keggin, J. F. *Nature* **1933**, *131*, 908. (b) Keggin, J. F. *Proc. R. Soc.* **1934**, *A144*, 75.
(12) Dawson, B. *Acta Crystallogr.* **1953**, *6*, 113.
(13) Weakley, T. J. R.; Finke, R. G. *Inorg. Chem.* **1990**, *29*, 1235.
(14) (a) Evans, H. T.; Tourné, C. M.; Tourné, G. F.; Weakley, T. J. R. *J. Chem. Soc., Dalton Trans.* **1986**, 2699. (b) Weakley, T. J. R.; Evans, H. T.; Showell, J. S.; Tourné, G. F.; Tourné, C. M. *J. Chem. Soc., Chem. Commun.* **1973**, 139.
(15) Finke, R. G.; Droege, M. W.; Domaille, P. J. *Inorg. Chem.* **1987**, *26*, 3886.

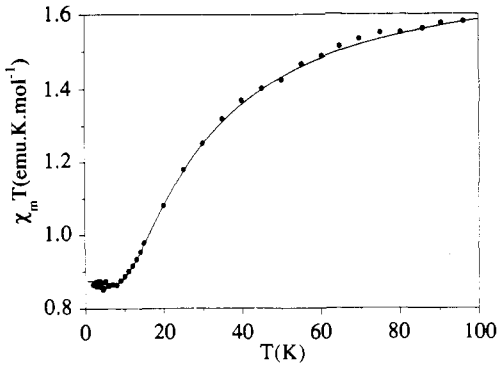

Figure 3. Plot of $\chi_m T$ versus T for the Dawson–Wells derivative copper compound II. The solid line represents the best fit from the Heisenberg exchange model.

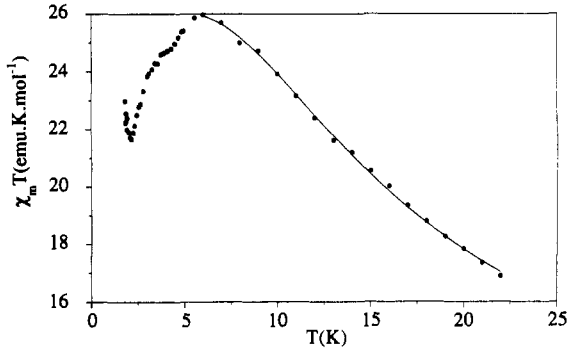

Figure 4. Plot of $\chi_m T$ versus T in the low-temperature region for the Keggin derivative cobalt compound III. The solid line represents the best fit from the anisotropic exchange model.

The magnetic measurements were carried out in the temperature range 2–298 K with a magnetometer (SHE/Co.) equipped with a SQUID sensor. Magnetization measurements at 2 and 5 K were carried out up to 50 kOe in the same apparatus. In the Cu(II) compounds I and II, the experimental susceptibility data were corrected for a temperature-independent paramagnetism of 7.0×10^{-4} emu/mol in I and 37.5×10^{-4} emu/mol in II. Such values had to be subtracted from the experimental susceptibility in order to obtain an approximately constant value of the $\chi_m T$ product at high temperatures (above 100 K) and account for diamagnetism of the samples and TIP contributions (of copper and tungsten). This result would indicate that in these compounds TIP contributions, arising mainly from W(VI), exceed diamagnetism. In fact, a positive value of $\chi_m = (10 \pm 2) \times 10^{-4}$ emu/mol is observed in the zinc compound $K_{10}[Zn_4(H_2O)_2(PW_9O_{34})_2]\cdot 20H_2O$. In the Co(II) compounds these corrections are negligible in the temperature range of interest (below 30 K) since, in this range of temperature, the experimental susceptibility data are larger than 4000×10^{-4} emu/mol. EPR spectra were recorded at X-band with a Bruker ER 200D spectrometer equipped with a helium cryostat.

Magnetic Results

Magnetic Properties of the Copper Clusters. The magnetic behaviors down to 2 K are plotted in Figures 2 and 3. The product $\chi_m T$ of the Keggin derivative (I) shows upon cooling a continuous decrease, reaching a minimum value of 0.86 emu mol^{-1} K below ca. 6 K (Figure 2). A very similar behavior is observed in the Dawson-Wells derivative (II) with a plateau of 0.87 emu mol^{-1} K at ca. 5 K (Figure 3). These behaviors are indicative of antiferromagnetic copper–copper interactions and suggest the presence of a magnetic $S = 1$ ground state in both cases.

Magnetic Properties of the Cobalt Clusters. The magnetic behavior of the Keggin derivative (III) is reported through a plot of the product $\chi_m T$ as a function of temperature in Figure 4. Upon cooling down, the product $\chi_m T$ shows a continuous increase below 30 K and a maximum at ca. 7 K; such features agree with the presence of intramolecular ferromagnetic cobalt–cobalt interactions. Below 7 K the product $\chi_m T$ shows a sharp decrease down to $T \approx 2$ K, followed by a sharp increase at lower temperatures; such features may result from the presence of intermolecular antiferromagnetic interactions. A very similar behavior is observed in the Dawson–Wells derivative (IV) (Figure 5).

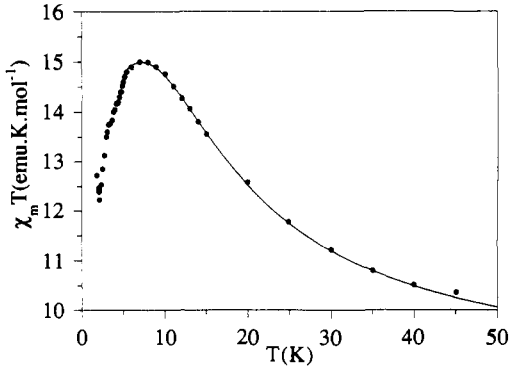

Figure 5. Plot of $\chi_m T$ versus T for the Dawson–Wells derivative cobalt compound IV. The solid line represents the best fit from the anisotropic exchange model.

Figure 6. EPR spectra of the 5% cobalt-doped Keggin derivative Zn compound at 4.2 K, $\{[Zn,Co]_4(H_2O)_2(PW_9O_{34})_2\}^{10-}$, showing the range of g values for the cobalt compounds.

Analyses of the Magnetic Interactions

Intracluster Interactions. Both Cu(II) and high-spin octahedral Co(II) can be described by a low-lying spin doublet $S = {}^1/_2$, which is almost isotropic in Cu(II) and anisotropic in Co(II). Notice that in Co(II) this effective spin doublet arises from the splitting of the $^4T_1$ term through spin–orbit coupling and local distortion of the octahedral sites.[16] In our case the anisotropy of the lowest Kramers doublet can be demonstrated from EPR measurements at 4.2 K on Co-doped samples of the corresponding heteropoly Zn compounds, which have shown g components in the range 2.6–7.0 (see Figure 6). On the other hand, the appearance of these spectra (as many as five signals can be distinguished) supports the presence of two different g tensors for the Co ions; that is in agreement with the two types of metal sites present in the cluster. As a consequence of the spin anisotropy of the Co ground state, a large anisotropy of the Co–Co interactions must be anticipated since this is given by $J_\perp/J_\parallel \approx (g_\perp/g_\parallel)^2$, where $J_\parallel$ and $J_\perp$ are the components parallel and perpendicular to the spin direction, respectively (for shake of simplicity, J has been assumed to be axial). The spin Hamiltonian appropriate for the exchange interaction of a four-spin $S = {}^1/_2$ rhomblike system, including the exchange anisotropy, can be written as

$$H = -2J_\parallel(S_{1z}S_{2z} + S_{2z}S_{3z} + S_{3z}S_{4z} + S_{1z}S_{4z}) - \\ -J_\perp(S_1^+S_2^- + S_1^-S_2^+ + S_2^+S_3^- + S_2^-S_3^+ + S_3^+S_4^- + S_3^-S_4^+ \\ + S_1^+S_4^- + S_1^-S_4^+) - 2J'_\parallel S_{2z}S_{4z} - J'_\perp(S_2^+S_4^- + S_2^-S_4^+) \quad (1)$$

where the numbering scheme is shown as follows:

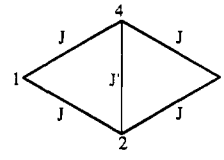

(16) Carlin, R. L. *Magnetochemistry*; Springer-Verlag: Berlin, 1986.

Table I. Magnetic Characterization of the M_4O_{16} (M = Co(II), Cu(II)) Clusters Encapsulated in Keggin and Dawson-Wells Derivatives

heteropolyanion	exchange params[a]	Landé params	ref
$[Cu_4(H_2O)_2(PW_9O_{34})_2]^{10-}$ (I)	$J = -3.5$ $J' = -12.5$	$g = 2.16$	10
$[Cu_4(H_2O)_2(P_2W_{15}O_{56})_2]^{16-}$ (II)	$J = -3.5$ $J' = -12.5$	$g = 2.16$	this work
$[Co_4(H_2O)_2(PW_9O_{34})_2]^{10-}$ (III)	$J_\parallel = 9.5 \pm 0.5$ $J_\perp/J_\parallel = 0.3$	$g_{\parallel a} = 6.1$, $g_{\perp a} = 5.1$ $g_{\parallel b} = 7.9$, $g_{\perp b} = 2.0$	9
$[Co_4(H_2O)_2(P_2W_{15}O_{56})_2]^{16-}$ (IV)	$J_\parallel = 10.5 \pm 0.5$ $J_\perp/J_\parallel = 0.4$	$g_{\parallel a} = 2.3$, $g_{\perp a} = 5.0$ $g_{\parallel b} = 7.9$, $g_{\perp b} = 2.9$	this work

[a] J values in cm^{-1}.

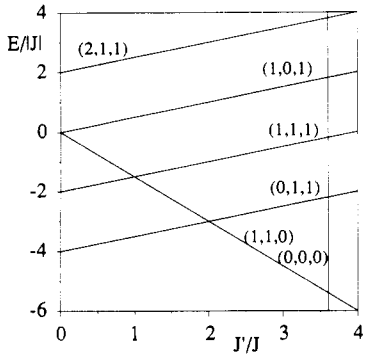

Figure 7. Energy levels diagram versus the ratio J'/J for the copper compounds from the fully isotropic Heisenberg exchange model (eq 2). Labels indicate (S, S^*, S^+) for each level, and the vertical line indicates the experimental J'/J value.

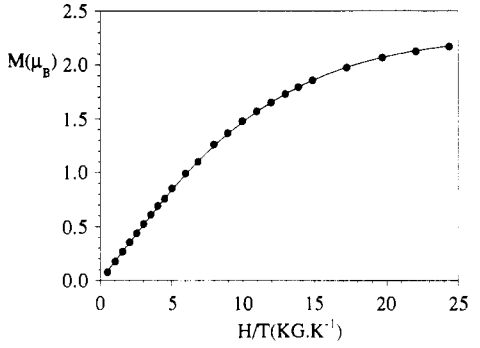

Figure 8. Magnetization data of the Keggin derivative copper compound I at 2 K. The solid line represents the behavior of two spins $S = {}^1/_2$ with a Landé factor $g = 2.28$.

In view of the symmetry of the tetramer, the four exchange interactions of the sides of the rhomb have been assumed to be identical (namely J), while that of the shortest diagonal of the rhomb may be different (namely J').

Copper Clusters. Owing to the isotropic ground state of the interacting copper ions, the magnetic behaviors are expected to be conveniently analyzed by the fully isotropic Heisenberg exchange model ($J_\parallel = J_\perp = J$; $J'_\parallel = J'_\perp = J'$). The total spin $S = S_1 + S_2 + S_3 + S_4$ is then a good quantum number, and so the vector-coupling method of Kambe[17] can be used to obtain the energies of the different spin states. There are two singlets, three triplets, and one quintet with energies

$$E(S,S^*,S^+) = -J[S(S+1) - S^*(S^*+1) - S^+(S^+ + 1)] - J'[S^+(S^+ + 1) - {}^3/_2] \quad (2)$$

In this expression, the energies are labeled using S, S^*, and S^+, where the total spin is given as $S = S^* + S^+$, $S^* = S_1 + S_3$, and $S^+ = S_2 + S_4$. In the antiferromagnetic case the energy level diagram vs the ratio J'/J is plotted in Figure 7. We notice that for a ratio $J'/J \geq 2$ the ground state of the cluster is formed by a triplet-spin state and a singlet one, even though both types of pairwise exchange interactions are antiferromagnetic. This intermediate-spin ground state results from spin frustration. In fact, this rhomblike arrangement can be viewed as being made up of two triangular units sharing a side. Similar situations have been previously found in manganese and iron clusters.[18] For $J'/J \leq 2$ the ground state of this cluster is $S = 0$. Thus, very different magnetic behaviors are to be expected depending on the ratio J'/J. Accordingly, for $J'/J \leq 2$, $\chi_m T$ would continuously decrease upon cooling, while for $J'/J \geq 2$ it would exhibit a minimum due to the irregular spin-state structure of the cluster[19] and a plateau at lower temperature, when only the ground state is populated. Compounds I and II do exhibit this type of behavior, indicating that the ground state of the Cu_4 clusters contains a spin-triplet. A very satisfying description of the experiment over the whole temperature range is obtained with the following set of parameters: $J = -3.5$ cm^{-1}, $J' = -12.5$ cm^{-1}, and $g = 2.16$, for both copper clusters (I and II). (These results are summarized in Table I).

The nature of the ground state of these clusters has been also characterized by magnetization measurements and powder EPR spectra. Thus, in view of the J'/J ratio, the ground state of the copper cluster is made of a spin-triplet and a spin-singlet located at the same energy. From a thermodynamic point of view, this situation is equivalent to that resulting from two independent spin-doublets. Accordingly, the magnetization data at 2 K have been fit by considering two spins $S = {}^1/_2$ in the theoretical expression of the magnetization:

$$M = N_A g \beta S B_s(y) \quad (3)$$

$$B_s(y) = (1/S)[(S + {}^1/_2) \coth ((S + {}^1/_2)y) - {}^1/_2 \coth ({}^y/_2)] \quad (4)$$

Here $B_s(y)$ is the Brillouin function of a spin S and $y = g\beta H/k_B T$. We obtain a very good agreement between theory and experiment when $g = 2.28$ (Figure 8). This result nicely supports the nature of the ground state deduced by magnetic susceptibility measurements. The calculated g value is somewhat larger than that obtained from the analysis of the susceptibility data. This may be due to the small thermal population of the low-lying excited levels of the cluster, which are not too far in energy from the ground state (the first excited state is at ca. 10 cm^{-1}).

On the other hand, the EPR spectra at 4.2 K of these compounds (Figure 9) are typical of spin-triplets with small values of the zero-field splitting parameters. In fact, spectra of both compounds (I and II) can be simulated from the following set of parameters: $|D| = 0.032 \pm 0.001$ cm^{-1}, $E/D = -0.17 \pm 0.01$, $g_x = 2.14 \pm 0.01$, $g_y = 2.03 \pm 0.01$, and $g_z = 2.24 \pm 0.01$. The assignation of bands is showed in Figure 9. The temperature dependence of the EPR spectra of the two compounds is very similar and is reported in Figure 10 for compound II. A significant variation above 30 K is observed, in agreement with the thermal population of the two excited triplet state which are lying at ca. 20 and 27 cm^{-1} above the ground triplet state.

Returning to the exchange values, their exact coincidence in the two copper compounds underlines the stability of the Cu_4 cluster in the solid state, independently of the heteropolytungstate. The reason that J' is stronger than J in both cases may be easily understood from the structural features of the tetramer. In this

(17) Kambe, K. *J. Phys. Soc. Jpn.* **1950**, *5*, 48.
(18) McCusker, J. K.; Schmitt, E. A.; Hendrickson, D. N. In *Magnetic Molecular Materials*; Gatteschi, D., Kahn, O., Miller, J., Palacio, F., Eds.; NATO ASI Series; Kluwer Academic Publishers: Dordrecht, The Netherlands, **1991**; Vol. 198 and references therein.
(19) Kahn, O. *Struct. Bonding* **1987**, *68*, 89.

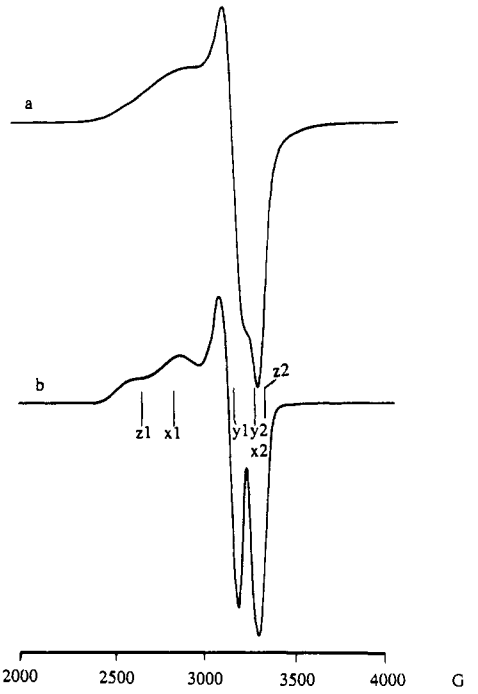

Figure 9. Polycrystalline powder EPR spectra at X-band of the two copper compounds at 4.2 K: (a) $[Cu_4(H_2O)_2(PW_9O_{34})_2]^{10-}$ (I); (b) $[Cu_4(H_2O)_2(P_2W_{15}O_{56})_2]^{16-}$ (II).

way, CuO_6 sites are distorted in such a way that the long axes of the four octahedra are parallel. Then, it is to be expected that the orbitals of Cu(II) containing the unpaired electron are disposed as schematized in Figure 1c. This situation favors the diagonal exchange interaction, J', with respect to the other interactions, since in this case the two $d_{x^2-y^2}$-type orbitals are pointing toward the bridging atoms, allowing for a larger overlap integral.

Cobalt Clusters. In view of the EPR results, an anisotropic exchange model with two different and anisotropic g tensors, $\mathbf{g}_a$ (for sites 1, 3) and $\mathbf{g}_b$ (for sites 2, 4) has been used in the analysis of the magnetic properties. Since in that case the total spin is not a good quantum number, a numerical procedure has been required to solve the exchange Hamiltonian.[9] Finally, in order to reduce the number of adjustable parameters, the five exchange interactions were set to be equal. The best fitted curves obtained by least-squares refinement of the magnetic data above 6 K are illustrated in Figures 4 and 5. The resulting parameters are listed in Table I. Several sets of parameters giving close agreement with the experiments have been found. Anyway, we have noticed that the exchange parameter $J_\parallel$ stays relatively constant in the fits independently of the amount of exchange anisotropy.[9] This indicates that magnetic measurements appear to be very useful to obtain reliable values for $J_\parallel$, but conversely, they are little sensitive to the amount of exchange anisotropy, $J_\perp/J_\parallel$. In order to study the exchange splitting in more detail, inelastic neutron scattering measurements on deuterated samples are in progress.

An unexpected result deals with the different sign of the exchange interactions in copper and cobalt compounds. In this respect it is to be noted that the interaction between orbitally degenerate ions, as for example high-spin cobalt(II) in octahedral sites, remains an essentially unsolved problem.[19] The high symmetry of this type of magnetic cluster and the small distortion of the octahedral CoO_6 sites should facilitate the theoretical treatment required to give a quantitative explanation of the ferromagnetic cobalt–cobalt interaction. In the following we present some simple ideas in order to qualitatively understand this result.

For the cobalt cluster, we can imagine two different types of exchange pathways, namely the superexchange paths involving the e_g-type orbitals and the bridging atoms and a direct exchange paths through the t_{2g}-type orbitals. With respect to the superexchange path, we observe that the M–O–M angles of the tetrameric entity, being 90 and ca. 100°, may favor a situation for accidental orthogonality of the e_g-type orbitals, and hence a ferromagnetic contribution might be expected. With respect to direct exchange pathways we notice that the geometry of the cluster, with coplanar metal ions sharing edges, could favor such exchange pathways (for example, the d_{xy}–d_{xy} pathway), since in this case the metallic centers are only separated by 3.16 and 3.19 Å.[14] In the framework of the Anderson model for the exchange[20] it is straightforward to see that, due to the orbital degeneracy of Co(II), these pathways might also stabilize a ferromagnetic ground state. That is so due to the possibility of having electronic transfers between t_{2g} orbitals of two interacting cobalts, keeping a parallel spin alignment in virtual Co(III)–Co(I) excited states. In this sense, it should be expected that the larger the overlap between these magnetic orbitals is, the stronger the ferromagnetic contribution. Quantitative calculations in other orbitally degenerate systems support this source of ferromagnetic coupling.[21] Such a result contrast with that obtained when the interaction between nondegenerate metal ions is considered, in which the overlap between the magnetic orbitals always favors the antiferromagnetic contribution, while the ferromagnetic situation is favored when this overlap is zero, due to the orbital orthogonality.[19]

Finally, it can be useful to mention an additional example of ferromagnetic interaction between Co(II) ions which has been reported by Losee et al.[22] in the linear chain $[(CH_3)_3NH]CoCl_3 \cdot 2H_2O$. It is interesting to note that the relevant exchange pathways of this compound are quite similar to those found in

Figure 10. Thermal variation of the EPR spectra of $[Cu_4(H_2O)_2(P_2W_{15}O_{56})_2]^{16-}$ (II): (a) T = 5.5 K; (b) T = 17 K; (c) T = 28 K; (d) T = 50 K; (e) T = 130 K; (f) T = 300 K.

(20) (a) Anderson, P. W. *Phys. Rev.* **1955**, *115*, 2. (b) Anderson, P. W. In *Magnetochemistry*; Rado, G. T., Suhl, H., Eds.; Academic Press: New York, 1963; Vol. I, Chapter 2.
(21) Drillon, M.; Georges, R. *J. Chem. Soc., Faraday Trans. 2* **1979**, *75*, 810.
(22) Losee, D. B.; McElearney, J. N.; Shankle, G. E.; Carlin, R. L.; Cresswell, P. J.; Robinson, W. T. *Phys. Rev. B* **1973**, *8*, 2185.

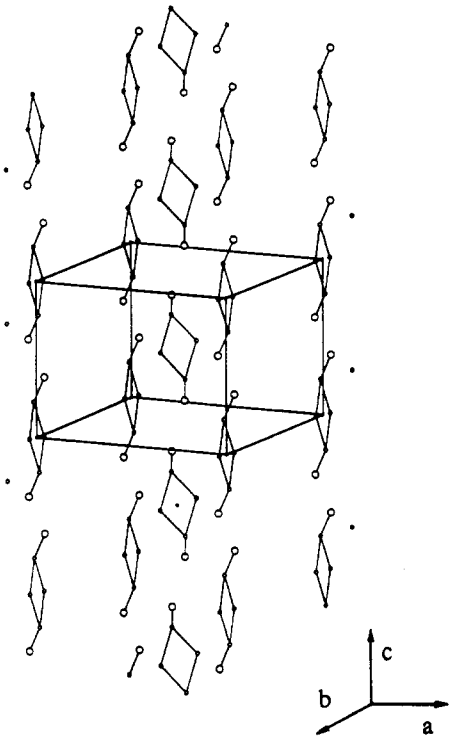

Figure 11. Structure of $[Co_4(H_2O)_2(PW_9O_{34})_2]^{10-}$ (III), showing the Co clusters and their connections along the *c*-axis.

the Co_4 cluster. Thus, although the Co–Cl–Co bridging angles and the distortions of the octahedral sites have changed (for example, the Co–Cl–Co bridging angles are 95 and 93° and the Co(II)–Co(II) distance is 3.64 Å), the presence of coplanar octahedral Co(II) ions sharing edges is still present.

Intercluster Interactions

Although in both copper and cobalt clusters the ground states are magnetic, only in the cobalt ones have the magnetic behaviors shown evidence of intercluster interactions. From the structural data on the Keggin derivatives we can notice that in both cases the shortest metal–metal distance is similar (7.62 Å in Cu and 7.15 Å in Co). However, the larger magnetic moment in the ground state of the Co clusters, together with the stronger intracluster exchange compared with that of the Cu clusters, may be at the origin of the larger intercluster interactions found in Co compounds. The arrangement of the clusters in the crystal lattice of the cobalt compound III shows that the clusters are forming one-dimensional arrays along the *c*-axis. In fact, each coordinated water molecule can interact with an oxygen bonded to a tungsten and with a coordinated water molecule of an adjacent anion (see Figure 11); the separation between the two oxygen atoms of these coordinated water molecules is 4.31 Å.

In the cobalt clusters, the presence of intercluster interactions becomes apparent from the comparison between the magnetization data at 2 and 5 K. As we can see from Figure 12, the saturation value decreases from ca. 12 μ_B at 5 K to ca. 9 μ_B at 2 K, suggesting that antiferromagnetic intercluster interactions are operative at the lower temperature. From the analysis of the magnetic susceptibility data the order of the energy levels gives a $M_s = \pm 2$/spin-doublet ground state for the Co_4 cluster, which is separated by ca. 20 cm^{-1} from the first excited state. Hence, the magnetization curve is expected to be that of an effective spin $S' = {}^1/_2$ with an effective Landé factor $g' = 4g_{Co}$. In Figure 12 we observe that the curve at $T = 5$ K fits reasonably well to the Brillouin function of a spin-doublet with $g' = 22$ (expression 2), which is in good agreement with the proposed ground state. Notice that the small differences between theory and experiment above $H/T \approx 5$ kG/K may arise as a consequence of the small thermal population of the excited levels of the cluster at this temperature. On the other hand, to account for the intercluster interactions, it may be assumed that they occur between the $S' = {}^1/_2$ ground

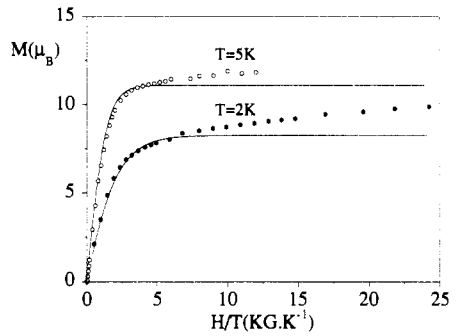

Figure 12. Magnetization data of the cobalt compound III at 2 and 5 K. At 2 K the experiment has been fitted to the magnetization of a Kramers spin doublet with $g = 22.2$ (eq 3). At 2 K the experiment has been reproduced from an $S = {}^1/_2$–two-sublattice Ising chain model with $g_1 = 22$, $g_2 = 11$, and $J = -0.6$ cm^{-1}.

states of the clusters. In view of the structural arrangement of the clusters in the lattice, the magnetic system may be then viewed as a chain of anisotropic spins $S' = {}^1/_2$. For an anisotropic Ising chain of spins $S = {}^1/_2$ formed by two magnetically nonequivalent sites, exact solutions for both parallel magnetization ($M_\parallel$) and susceptibility ($\chi_\parallel$) have been derived.[23] Parallel in this context means that the external magnetic field is assumed to be along the quantization axis. From these expressions we have estimated the order of magnitude of the intercluster interactions. Thus, the magnetization data at 2 K have been fit from the following set of parameters: $g_1 = 22$, $g_2 = 11$, $J = -0.3$ cm^{-1} (solid line of Figure 12). The resulting *g* values are different and account for the different orientations of the **g** tensors of two nearest-neighbor clusters with respect to the quantization axis. Dealing with the low-temperature magnetic susceptibility data, a two-sublattice Ising model is also required in order to explain the minimum of $\chi_m T$ at ca. 2 K, which is the typical feature of a 1-d ferrimagnet. We obtain values of the exchange interaction ranging from −0.6 to −2 cm^{-1}. Emphasis is placed on the fact that intercluster interactions extending in one dimension have to be considered to account for the low-temperature magnetic data, rather than for the values indicated. Thus, these results indicate that intercluster interactions are 1 order of magnitude smaller than the intracluster ones.

Concluding Remarks

We have reported here four examples of tetrametallic exchange-coupled systems isolated in heteropolymolecules. With respect to the intracluster interactions, very good agreements of the experimental data have been obtained by assuming isotropic and antiferromagnetic (Cu_4 clusters) or anisotropic and ferromagnetic (Co_4 clusters) exchange interactions within the molecular entities.

On the other hand, the ideal isolation provided by the heteropolytungstate framework has guaranteed the intramolecular nature of the exchange interaction in the copper clusters, for which no sign of intercluster interactions has been detected from both magnetic susceptibility and magnetization data. Conversely, in the cobalt clusters the structural arrangement of the molecules has favored the presence of exchange-coupled chains of Co_4 clusters. Antiferromagnetic intercluster interactions 1 order of magnitude smaller than the intracluster ones have been estimated from magnetic susceptibility and magnetization data.

Finally, the magnetic nature of the ground states of these anions, together with their stability in solution as well as in the solid state, make these molecules suitable as building blocks of extended magnetic structures. We hope that the association of this kind of molecule with suitably chosen cations (as for example organic radicals of the type TTF and derivatives) results in the develop-

(23) (a) Coronado, E.; Drillon, M.; Nugteren, P. R.; de Jongh, L. J.; Beltran, D.; Georges, R. *J. Am. Chem. Soc.* **1988**, *110*, 3907. (b) Coronado, E.; Drillon, M.; Nugteren, P. R.; de Jongh, L. J.; Beltran, D.; Georges, R. *J. Am. Chem. Soc.* **1989**, *111*, 3874.

ment of new molecular magnetic materials with interesting properties or combination of properties. Attempts are in progress.

Acknowledgment. This work was supported by the Comisiõn Interministerial de Ciencia y Tecnologia (Grant MAT89-177), by the Spanish-French Integrated Action TM-189, and by the Institució Valenciana d'Estudis i Investigació. We are deeply grateful to the Centre de Recherches Paul Pascal (Talence, France) for allowing us the use of the SQUID magnetometer and to C. Zanchini from the Dept di Chimica of Florence for her help in the low-temperature EPR measurements. It is a pleasure to acknowledge enthusiastic discussions with Prof. L. C. W. Baker in the exciting area of polyoxoanions. C.J.G.-G. and J.J.B.-A. thanks the Ministerio de Educaciõn y Ciencia for a grant. E.C. thanks the Generalitat Valenciana for a travel grant.

Registry No. I, 98773-81-0; II, 97836-72-1; III, 98743-06-7; IV, 97836-71-0.

Contribution from the Departments of Chemistry, University of California, San Diego, La Jolla, California 92093-0314, and University of Missouri, Columbia, Missouri 65211

Synthesis and Structures of the Bis(*cis*-1-methylthiostilbene-2-thiolate) of Cadmium and Its Adducts with Dimethyl Sulfoxide, 4-(Dimethylamino)pyridine, and 2,2′-Bipyridyl: Hexacoordination of Cadmium vs Pentacoordination in the Corresponding Zinc Derivatives

Hussain K. Reddy,[†] Cheng Zhang,[‡] E. O. Schlemper,*[,§] and G. N. Schrauzer*[,∥]

Received August 19, 1991

Whereas the zinc derivative of *cis*-1-methylthiostilbene-2-thiol forms a well-defined μ-S-bridged dimer of composition $Zn_2[Ph(SCH_3)C{=}C(S)Ph]_4$ with pentacoordinated zinc, the corresponding compound of cadmium appears to have a polymeric structure. However, it forms a well-defined μ-S-bridged dimeric 1:1 adduct with dimethyl sulfoxide (DMSO), $Cd[Ph(SCH_3)C{=}C(S)Ph]_2(DMSO)$, of composition $C_{32}H_{32}S_5CdO$, with hexacoordinated cadmium, crystallizing in the triclinic space group $P\bar{1}$ with unit cell parameters a = 11.529 (4) Å, b = 12.955 (5) Å, c = 22.804 (8) Å, α = 106.480 (20)°, β = 92.590 (20)°, and γ = 94.680 (20)°, with Z = 2. The coordination geometry of the cadmium ions is distorted octahedral, the DMSO is coordinated via oxygen, and the Cd–O bond length is 2.358 (6) Å. The sulfur ligands are bound in an anisobidentate fashion, with normal covalent Cd–S and Cd–μ-S bonds of 2.5072 (22) and 2.6364 (22) Å and elongated coordinative Cd–S bonds of 2.8045 (22) and 2.976 (3) Å, respectively. On reaction with 4-(dimethylamino)pyridine (dmapy), a hexacoordinated 1:2 adduct, $Cd[Ph(CH_3S)C{=}C(S)Ph]_2(dmapy)_2$, of composition $C_{44}H_{46}N_2S_4Cd$ is formed, which crystallizes in the monoclinic space group $C2/c$ with a = 17.483 (4) Å, b = 12.290 (3) Å, c = 19.963 (5) Å, β = 98.998 (20)°, and Z = 4. The mean covalent Cd–S and coordinate Cd–N bond distances of 2.556 (1) Å and 2.384 (4) Å are within normal ranges, and the mean coordinate Cd–S bonds of 2.869 (2) Å are elongated but genuine coordinate bonds. The coordination geometry of Cd is distorted octahedral, and the dmapy molecules are in cis positions opposing the coordinate Cd–S bonds. The adduct with 2,2′-bipyridyl (bpy), $Cd[Ph(SCH_3)C{=}C(S)Ph]_2(bpy)$, of composition $C_{40}H_{34}N_2S_4Cd$, also contains hexacoordinated Cd and crystallizes in the triclinic space group $P\bar{1}$, with a = 13.652 (3) Å, b = 12.843 (7) Å, c = 10.5640 (20) Å, α = 101.39 (3)°, β = 94.200 (20)°, γ = 94.36 (3)°, and Z = 2. The mean covalent and mean coordinate Cd–N bond lengths of 2.5260 (13) and 2.382 (36) Å are normal; the coordinate Cd–S bonds of 2.8151 (19) Å are elongated due to the anisobidentate attachment of the sulfur ligands. Cadmium ions thus have a greater tendency to adopt higher coordination numbers than zinc, which could account for some of the reactivity differences between the two elements in biological systems.

Introduction

In recent paper,[1] we showed that the zinc derivative of *cis*-1-methylthiostilbene-2-thiol, $Zn[Ph(SCH_3)C{=}C(S)Ph]_2$ and its adducts with 4-(dimethylamino)pyridine (dmapy) and 2,2′-bipyridyl (bpy) adopt pentacoordinated structures under conditions where tetra- and hexacoordinated geometries are possible. This observation may be relevant to the understanding of the functions of zinc in enzymes and in other biologically important zinc complexes in which zinc is usually assumed to be tetracoordinated. While this is often true for the resting states of the enzymes, it need not necessarily be the case, especially not in their functional states. Thus, in enzymes such as carbonic anhydrase[2] and in liver alcohol dehydrogenase,[3] zinc has been assumed to be pentacoordinated. Complexes of zinc with coordination numbers higher than 4 may also be formed in the interactions of the complexed zinc ions in the RNA and DNA polymerases with the base components of the nucleic acids.[4] Much of this evidence was obtained through studies of the enzymes in which zinc was substituted by cobalt[5] or cadmium[6] and from work with model compounds of these elements. In the previously investigated complexes with simple thiolato and nitrogen ligands, tetracoordination predominated, but the number of cases investigated is still relatively small. We therefore decided to synthesize the cadmium derivatives of *cis*-1-methylthiostilbene-2-thiol and of their adducts with dmapy and bpy and to compare their structures with those of the corresponding zinc compounds.

In contrast to the dimeric Zn derivative, the corresponding Cd complex of composition $Cd[Ph(SCH_3)C{=}C(S)Ph]_2$ (**1**) was found to be only marginally soluble in common solvents, suggesting a polymeric structure. On reaction of **1** with dimethyl sulfoxide (DMSO), however, a crystalline adduct of composition $Cd[Ph(SCH_3)C{=}C(S)Ph]_2$ (DMSO) (**2**) was obtained which could be structurally characterized. In further contrast to the behavior

[†] Present address: Department of Chemistry, Sri Krishnadevaraya University, Anantapur, 515003 India.
[‡] Present address: Department of Chemistry, Massachusetts Institute of Technology, Cambridge, MA 02139.
[§] University of Missouri.
[∥] University of California.

(1) Zhang, C.; Chadha, R.; Reddy, H. K.; Schrauzer, G. N. *Inorg. Chem.* **1991**, *30*, 3865.
(2) (a) Gupta, R. K.; Pesando, J. M. *J. Biol. Chem.* **1975**, *250*, 2630. (b) Kannan, K. K.; Pelef, M.; Fridbourg, K.; Cid-Dresner, M.; Lougren, S. *FEBS Lett.* **1977**, *73*, 115.
(3) Dworschach, R. T.; Plapp, B. V. *Biochemistry* **1977**, *16*, 2716.
(4) Wu, F. Y.-H.; Wu, Ch.-W. *Annu. Rev. Nutr.* **1987**, *7*, 251-272 and references cited therein.
(5) Corwin, D. T., Jr.; Fikar, R.; Koch, S. A. *Inorg. Chem.* **1987**, *26*, 3080.
(6) Corwin, D. T., Jr.; Gruff, E. S.; Koch, S. A. *J. Chem. Soc., Chem. Commun.* **1987**, 966.

0020-1669/92/1331-1673$03.00/0